Halogen-free chelated orthoborate ionic liquids and organic ionic plastic crystals

ARTICLE *in* JOURNAL OF MATERIALS CHEMISTRY · JANUARY 2012

Impact Factor: 7.44 · DOI: 10.1039/C2JM12657E

Journal of Materials Chemistry

Dynamic Article Links

Cite this: *J. Mater. Chem.*, 2012, **22**, 6928

www.rsc.org/materials

PAPER

Halogen-free chelated orthoborate ionic liquids and organic ionic plastic crystals†

Faiz Ullah Shah,[a] Sergei Glavatskih,[b] Pamela M. Dean,[c] Douglas R. MacFarlane,[c] Maria Forsyth[de] and Oleg N. Antzutkin*[af]

Received 9th June 2011, Accepted 23rd January 2012
DOI: 10.1039/c2jm12657e

Five halogen-free orthoborate salts comprised of three different cations (cholinium, pyrrolidinium and imidazolium) and two orthoborate anions, bis(mandelato)borate and bis(salicylato)borate, were synthesised and characterised by DSC, X-ray diffraction and NMR. DSC measurements revealed that glass transition points of these orthoborate salts are in the temperature range from −18 to −2 °C. In addition, it was found that [EMPy][BScB] and [EMIm][BScB] salts have solid–solid phase transitions below their melting points, *i.e.* they exhibit typical features of plastic crystals. Salts of the bis(salicylato) borate anion $[BScB]^-$ have higher melting points compared with corresponding salts of the bis(mandelato)borate anion $[BMB]^-$. Single crystal X-ray diffraction crystallography (for [Chol][BScB] crystals) and solid-state multinuclear (^{13}C, ^{11}B and ^{15}N) NMR spectroscopy were employed for the structural characterisation of [Chol][BScB], [EMPy][BScB] and [EMIm][BScB], which are solids at room temperature: a strong interaction between $[BScB]^-$ anions and $[Chol]^+$ cations was identified as (i) hydrogen bonding between OH of $[Chol]^+$ and carbonyl groups of $[BScB]^-$ and (ii) as the inductive C–H$\cdots\pi$ interaction. In the other salt, [EMIm][BScB], anions exhibit $\pi\cdots\pi$ stacking in combination with C–H$\cdots\pi$ interactions with $[EMIm]^+$ cations. These interactions were not identified in [EMPy][BScB] probably because of the lack of aromaticity in cations of the latter system. Our data on the formation of a lanthanum complex with bis(salicylato)borate in the liquid mixture of La^{3+}(aq) with [Chol][BScB] suggest that this class of novel ILs can be potentially used in the extraction processes of metal ions of rare earth elements.

1. Introduction

Ionic liquids (ILs) have attracted the interest of many researchers because of their unique properties that make them useful in a wide range of applications.[1] Some of their properties include favorable solubility of organic and inorganic compounds, relatively high ionic conductivity, low vapour pressure, high thermal stability and low flammability.[2–4] These unique properties open a gateway for new applications and improvements of existing technologies.[5] ILs are already widely used in organic synthesis,[6,7] catalysis,[8–10] electrochemistry,[11–13] recyclable solvents for organic reactions and separation processes,[14,15] active pharmaceutical ingredients,[16,17] extraction of lanthanide and other metal ions,[18–20] and functional materials.[21–23]

Most known ionic liquids (ILs) are composed of organic cations, for example, imidazolium, pyridinium, pyrrolidinium, ammonium, and phosphonium, and inorganic anions such as tetrafluoroborate, hexafluorophosphate and bis(trifluoromethylsulfonyl)imide. Note that over 10^{18} simple organic salts that might be potential ILs can be designed by varying the substitution patterns and choice of anions.[24] In such a design one can aim at specific interactions between cations and anions that result in desired properties of ILs. Such interactions include Coulomb forces, dispersive and inductive interactions, $\pi\cdots\pi$ stacking (often in aromatic systems), hydrogen bonding and hydrogen-bond-like interactions.[25] It is generally believed that

[a]*Chemistry of Interfaces, Luleå University of Technology, SE-97 187 Luleå, Sweden. E-mail: Oleg.Antzutkin@ltu.se; O.N.Antzutkin@warwick.ac.uk*
[b]*System and Component Design, KTH, Royal Institute of Technology, SE-10 044 Stockholm, Sweden*
[c]*School of Chemistry, Monash University, Clayton, Victoria 3800, Australia*
[d]*Department of Materials Engineering, Monash University, Clayton, Victoria 3800, Australia*
[e]*Institute for Technology Research and Innovation and Centre for Material and Fibre Innovation, Deakin University, Geelong, Victoria 3217, Australia*
[f]*Department of Physics, University of Warwick, CV4 7AL Coventry, UK*

† Electronic supplementary information (ESI) available: ESI-MS and (^1H, ^{13}C, and ^{11}B) NMR spectra in $CDCl_3$ of all the synthesised halogen-free chelated orthoborate ionic liquids and plastic crystals; crystallographic data for [Chol][BScB]; ^{15}N CSA analysis for [EMIm][BScB]; ^{13}C CP/MAS NMR spectrum of a powder lanthanum complex with bis(salicylato)borate after the extraction process of La^{3+}(aq) by [Chol][BScB]. CCDC reference number 809334. For ESI and crystallographic data in CIF or other electronic format see DOI: 10.1039/c2jm12657e

Coulomb interactions dominate the properties of ILs because of their ionic nature. However, hydrogen bonding also plays a significant role in the cation–anion interactions, structure and organisation of ILs in both solid and liquid phases.[26–28] In particular, these interactions between cations and anions have been extensively studied in imidazolium based ILs and correlated with their physicochemical properties.[29–31]

It is worth noting that, despite their attractive properties, water soluble ILs are undesirable in many practical applications due to their environmental problems and potential toxicity. In particular, ILs containing halogenated anions, such as PF_6^- and BF_4^-, may also produce corrosive species such as HF and other highly reactive acidic products following hydrolysis of these anions.[32–34] In addition, accumulation in nature and disposals of halogen-based ionic liquids may cause severe environmental problems. Therefore, the design of halogen-free and hydrolytically stable anions is one of the possible ways to avoid the liberation of corrosive and toxic ILs and products of their decomposition into the environment, in particular, when ILs are and will be widely used in different high-technology applications.[35] Recently, a number of studies have shown that even cationic moieties of ILs may have potential environmental problems and toxicity in nature.[36–39] Docherty and Kulpa have measured the toxicity and antimicrobial activity of a series of imidazolium and pyridinium ILs containing bromide and dicyanamide anions and have found that cations with longer alkyl chains are more toxic than cations with shorter ones.[40] Therefore, the design of novel functionalised ILs, which can replace the potentially toxic halogenated ILs in a wide range of applications, is of great significance.

We have recently reported that halogen-free and hydrolytically stable chelated orthoborate ILs (hf-BILs) with phosphonium cations, which are liquids at room temperature, are promising future lubricants, which outperform commercial fully formulated mineral oils for steel–aluminium alloy contacts.[41] In this work, we report on the synthesis, physical and structural characterisation of a family of novel halogen-free salts based on orthoborate anions (bis(salicylato)borate, $[BScB]^-$, and bis(mandelato)borate, $[BMB]^-$) and different nitrogen based cations with short alkyl chains. Unlike the previously studied room temperature orthoborate–phosphonium based ILs,[41] these new salts are either solids (with $[BScB]^-$) or viscous liquids (with $[BMB]^-$) at room temperature. Multinuclear (^{13}C, ^{11}B and ^{15}N) solid-state NMR spectroscopy was used to study interactions between cations and anions in the novel salts, which are solids at ambient temperatures: a representative cation from several of the classic families such as $[Chol]^+$, $[EMPy]^+$ and $[EMIm]^+$ was selected, in combination with the common $[BScB]^-$ anion. [Chol][BScB] crystals suitable for X-ray diffraction were prepared and the single crystal structure of this salt was successfully solved. Some of the new salts have shown characteristic features of plastic crystals which, when doped with a lithium salt, are potential candidates for higher temperature lithium battery systems.[42,43] In addition, it was also found that [Chol][BScB] IL readily forms a complex with lanthanum and thus this (and other ILs belonging to the same class) can be potentially used in the extraction processes of rare earth elements from aqueous solutions.

2. Experimental section

2.1 Chemicals

Boric acid (BDH, 99.8% purity), lithium carbonate (Aldrich, 99.99% purity), mandelic acid (Merck, for synthesis), salicylic acid (UNILAB Australia, >99.5% purity), 1-methylpyrrolidine (ACROS Organics, 98% purity), 1,2-dimethylimidazole (ACROS Organics, 98% purity), iodoethane (Sigma-Aldrich, 99% purity), choline chloride and dichloromethane were used as received.

2.2 Synthesis

N-Ethyl-*N*-methylpyrrolidinium iodide [EMPy]I and 1-ethyl-2,3-dimethylimidazolium iodide [EMIm]I were synthesised using the reported method.[44] Orthoborate salts were synthesised by using slightly modified literature methods.[45,46]

2.2.1 1-Ethyl-2,3-dimethylimidazolium bis(mandelato)borate [EMIm][BMB]. Mandelic acid (3.043 g, 20 mmol) was added slowly to an aqueous solution of lithium carbonate (0.369 g, 5 mmol) and boric acid (0.618 g, 10 mmol) in 50 mL water. The solution was heated up to about 60 °C for two hours. The reaction was cooled to room temperature and 1-ethyl-2,3-dimethylimidazolium iodide (2.52 g, 10 mmol) was added. The reaction mixture was stirred for two hours at room temperature. The bottom layer of the reaction product formed was extracted with 80 mL of CH_2Cl_2. The CH_2Cl_2 organic layer was washed three times with 100 mL water. The CH_2Cl_2 was rotary evaporated at reduced pressure and the final product was dried in a vacuum oven at 60 °C for 2 days. A viscous ionic liquid was obtained in 78% yield (3.40 g).

MS (ESI) calcd for $[C_7H_{13}N_2]^+$ *m*/*z* 125.2; found *m*/*z* 125.2; calcd for $[C_{16}H_{12}O_6B]^-$ *m*/*z* 311.0; found *m*/*z* 311.1.

Anal. calcd for $C_{23}H_{25}O_6N_2B$, $M_w = 436.246$ g mol^{-1}: C, 63.3; H, 5.8; N, 6.4. Found: C, 61.9; H, 5.7; N, 6.0%.

^1H NMR (400.17 MHz, $CDCl_3$): 7.554–7.498 (m, 4H, C_6H_5), 7.292–7.244 (m, 4H, C_6H_5), 7.236–7.182 (m, 2H, C_6H_5), 6.78 (d, 1H, $^3J_{HH} = 2.0$ Hz, NCH), 6.75 (d, 1H, $^3J_{HH} = 2.4$ Hz, NCH), 5.237 (s, 1H, C_6H_5-C*H*), 5.188 (s, 1H, C_6H_5-C*H*), 3.716 (q, 2H, $^3J_{HH} = 7.2$ Hz, CH_2-CH_3), 3.349 (s, 3H, CH_3), 2.183 (s, 3H, CH_3), 1.161 (t, 3H, $^3J_{HH} = 7.2$ Hz, CH_2-CH_3) ppm.

^{13}C NMR (100.62 MHz, $CDCl_3$): 177.89, 177.82, 142.98, 140.06, 134.86, 128.86, 128.40, 127.52, 126.66, 126.26, 122.23, 119.87, 43.45, 34.85, 14.44, 9.04 ppm.

^{11}B NMR (129.39 MHz, $CDCl_3$): 10.71 ppm.

2.2.2 1-Ethyl-2,3-dimethylimidazolium bis(salicylato)borate [EMIm][BScB]. The procedure is similar to that used in the synthesis of [EMIm][BMB]. The reaction started with lithium carbonate (0.369 g, 5 mmol), boric acid (0.618 g, 10 mmol), salicylic acid (2.762 g, 20 mmol) and 1-ethyl-2,3-dimethylimidazolium iodide (2.52 g, 10 mmol). A white solid product was obtained in 83% yield (3.38 g).

MS (ESI) calcd for $[C_7H_{13}N_2]^+$ *m*/*z* 125.2; found *m*/*z* 125.1; calcd for $[C_{14}H_8O_6B]^-$ *m*/*z* 283.0; found *m*/*z* 283.0.

Anal. calcd for $C_{21}H_{21}O_6N_2B$, $M_w = 408.232$ g mol^{-1}: C, 61.8; H, 5.2; N, 6.8. Found: C, 61.7; H, 5.1; N, 6.3%.

^{1}H NMR (400.17 MHz, $CDCl_3$): 7.770 (dd, 2H, $^3J_{HH} = 6.0$ Hz, $^4J_{HH} = 2.0$ Hz, C_6H_4), 7.353–7.310 (m, 2H, C_6H_4), 6.999 (d, 1H, $^3J_{HH} = 2.4$ Hz, NCH), 6.971 (d, 1H, $^3J_{HH} = 2.0$ Hz, NCH), 6.850–6.791 (m, 4H, C_6H_4), 3.880 (q, 2H, $^3J_{HH} = 7.2$ Hz, N-CH_2-CH_3), 3.554 (s, 3H, N-CH_3), 2.379 (s, 3H, CH_3), 1.242 (t, 3H, $^3J_{HH} = 7.2$ Hz, CH_2-CH_3) ppm.

^{13}C NMR (100.62 MHz, $CDCl_3$): 165.04, 159.0, 134.62, 129.24, 122.25, 119.77, 118.91, 116.97, 114.95, 43.35, 34.80, 14.22, 8.97 ppm.

^{11}B NMR (129.39 MHz, $CDCl_3$): 3.31 ppm.

2.2.3 *N*-Ethyl-*N*-methylpyrrolidinium bis(mandelato)borate [EMPy][BMB]. The procedure is similar to that used in the synthesis of [EMIm][BMB]. The reaction started with lithium carbonate (0.369 g, 5 mmol), boric acid (0.618 g, 10 mmol), mandelic acid (3.043 g, 20 mmol) and *N*-ethyl-*N*-methylpyrrolidinium iodide (2.41 g, 10 mmol). A viscous ionic liquid was obtained in 67% yield (2.85 g).

MS (ESI) calcd for $[C_6H_{16}N]^+$ *m*/*z* 114.2; found *m*/*z* 114.1; calcd for $[C_{16}H_{12}O_6B]^-$ *m*/*z* 311.0; found *m*/*z* 311.0.

Anal. calcd for $C_{22}H_{28}O_6NB$, $M_w = 413.303$ g mol^{-1}: C, 63.9; H, 6.8; N, 3.4. Found: C, 63.6; H, 6.6; N, 3.4%.

^{1}H NMR (400.17 MHz, $CDCl_3$): 7.582–7.540 (m, 4H, C_6H_5), 7.324–7.271 (m, 4H, C_6H_5), 7.261–7.216 (m, 2H, C_6H_5), 5.308 (s, 1H, C_6H_5-C*H*), 5.263 (s, 1H, C_6H_5-C*H*), 3.049–2.982 (m, 4H, N-CH_2-), 2.945 (q, 2H, $^3J_{HH} = 7.2$ Hz, N-CH_2-CH_3), 2.358 (s, 3H, N-CH_3), 1.852–1.768 (m, 4H, -CH_2-), 1.00 (t, 3H, $^3J_{HH} = 7.2$ Hz, CH_2-CH_3) ppm.

^{13}C NMR (100.62 MHz, $CDCl_3$): 178.09, 178.01, 139.99, 139.92, 133.13, 130.07, 128.87, 128.37, 127.62, 126.68, 126.34, 63.67, 59.45, 47.39, 21.31, 8.95 ppm.

^{11}B NMR (129.39 MHz, $CDCl_3$): 10.84 ppm.

2.2.4 *N*-Ethyl-*N*-methylpyrrolidinium bis(salicylato)borate [EMPy][BScB]. The procedure is similar to that used in the synthesis of [EMIm][BMB]. The reaction started with lithium carbonate (0.369 g, 5 mmol), boric acid (0.618 g, 10 mmol), salicylic acid (2.762 g, 20 mmol) and *N*-ethyl-*N*-methylpyrrolidinium iodide (2.41 g, 10 mmol). A white solid product was obtained in 78% yield (3.1 g).

MS (ESI) calcd for $[C_6H_{16}N]^+$ *m*/*z* 114.2; found *m*/*z* 113.9; calcd for $[C_{14}H_8O_6B]^-$ *m*/*z* 283.0; found *m*/*z* 283.0.

Anal. calcd for $C_{20}H_{24}O_6NB$, $M_w = 385.245$ g mol^{-1}: C, 62.4; H, 6.3; N, 3.6. Found: C, 63.4; H, 6.0; N, 3.4%.

^{1}H NMR (400.17 MHz, $CDCl_3$): 7.849 (dd, 2H, $^3J_{HH} = 6.0$ Hz, $^4J_{HH} = 2.0$ Hz, C_6H_4), 7.412–7.357 (m, 2H, C_6H_4), 6.888–6.848 (m, 4H, C_6H_4), 3.328–3.275 (m, 4H, N-CH_2-), 3.239 (q, 2H, $^3J_{HH} = 7.2$ Hz, N-CH_2-CH_3), 2.825 (s, 3H, N-CH_3), 2.012–1.978 (m, 4H, -CH_2-), 1.149 (t, 3H, $^3J_{HH} = 7.2$ Hz, CH_2-CH_3) ppm.

^{13}C NMR (100.62 MHz, $CDCl_3$): 165.64, 159.31, 135.13, 129.64, 119.38, 119.20, 118.41, 115.21, 63.90, 59.65, 47.70, 21.49, 9.07 ppm.

^{11}B NMR (129.39 MHz, $CDCl_3$): 3.49 ppm.

2.2.5 Choline bis(salicylato)borate [Chol][BScB]. The procedure is similar to that used in the synthesis of [EMIm][BMB]. The reaction started with lithium carbonate (0.369 g, 5 mmol), boric acid (0.618 g, 10 mmol), salicylic acid (2.762 g, 20 mmol) and choline chloride (1.39 g, 10 mmol). A white solid product was obtained in 70% yield (2.72 g).

MS (ESI) calcd for $[C_5H_{14}NO]^+$ *m*/*z* 104.1; found *m*/*z* 103.9; calcd for $[C_{14}H_8O_6B]^-$ *m*/*z* 283.0; found *m*/*z* 283.0.

Anal. calcd for $C_{19}H_{22}O_7NB$, $M_w = 387.214$ g mol^{-1}: C, 58.9; H, 5.7; N, 3.6. Found: C, 59.1; H, 5.5; N, 3.2%.

^{1}H NMR (400.17 MHz, $CDCl_3$): 10.50 (s, 1H, OH), 7.838 (dd, 2H, $^3J_{HH} = 6.4$ Hz, $^4J_{HH} = 1.6$ Hz, C_6H_4), 7.408–7.365 (m, 2H, C_6H_4), 6.915–6.844 (m, 4H, C_6H_4), 3.921–3.884 (m, 2H, -CH_2-O), 3.365–3.341 (m, 2H, N-CH_2-), 3.019 (s, 9H, N-CH_3) ppm.

^{13}C NMR (100.62 MHz, $CDCl_3$): 165.49, 159.31, 135.62, 129.72, 119.42, 118.58, 117.56, 114.73, 68.04, 56.24, 54.53, 54.49, 54.46 ppm.

^{11}B NMR (129.39 MHz, $CDCl_3$): 3.54 ppm.

2.3 Extraction of lanthanum by [Chol][BScB] from aqueous solution

[Chol][BScB] (0.387 g, 1 mmol) was added to an aqueous solution of lanthanum nitrate hexahydrate (0.433 g, 1 mmol) in 20 mL of Milli-Q water. The suspension was heated at reflux temperature (*ca.* 90 °C) and a clear solution was obtained after 2 hours. The heating was continued for 6 more hours and the precipitate formed was filtered and dried. The precipitate was not soluble in common organic solvents. It was characterised by ICP-SFMS and ^{11}B MAS and ^{13}C CP/MAS NMR. ICP-MS analysis has shown that the precipitate contains 3400 mg kg^{-1} of boron (0.34 wt%) and 66 000 mg kg^{-1} of lanthanum (6.6 wt%). Solid-state NMR data of the precipitate are discussed below in "Results and Discussion".

2.4 Physical characterisation

The C, H and N elemental analysis for ILs was performed according to the Dumas method using a Flash EA 1112 from Thermo Finnigan elemental analyser in Mikro Kemi AB Uppsala.[47] About 1 mg of the sample was weighed in a tin capsule, sealed and placed in an autosampler, from which it was dropped into a combustion chamber. As the sample entered the combustion chamber oxygen was injected into the carrier gas (He), which flowed through the combustion tube. The temperature was raised to 1800 °C, which ensured complete combustion of the sample. Detection was done with a hot wire detector. Quantification was accomplished using certified external standards and the method of least squares with correlation coefficient >0.999.

The precipitate obtained in the reaction of [Chol][BScB] with La^{3+}(aq) was analysed by ICP-SFMS in ALS global laboratory group Luleå (for the elemental analysis of lanthanum and boron).[48] Approximately 50 mg of the sample was digested with 1 mL concentrated HNO_3 (MW-assisted digestion in closed Teflon vessels). After cooling to room temperature the digest was diluted with Milli-Q water and concentrations of lanthanum and boron were determined using a combination of internal standardization and external calibration. The elemental analysis was carried out in the medium resolution range, $\Delta m/m \approx 4500$ (Finnigan MAT, Bremen, Germany). Each measurement was done in triplicate.

Liquid-state NMR experiments were carried out on a Bruker Avance 400 ($B_0 = 9.4$ T) with a 5 mm broadband auto-tunable probe with *Z*-gradients at 30 °C. NMR spectra were collected

and processed using spectrometer "Topspin" 2.1 software. ^{1}H (400.17 MHz) and ^{13}C (100.63 MHz) NMR spectra were referenced to internal TMS and $CDCl_3$. An external reference ($Et_2O \cdot BF_3$) was employed in ^{11}B (128.39 MHz) NMR spectra.[49]

Solid-state multinuclear (^{13}C, ^{11}B and ^{15}N) magic-angle-spinning (MAS) NMR spectra of solid salts were recorded either on an Agilent/Varian/Chemagnetics InfinityPlus CMX-300 (B_0 = 7.05 T, 75.47 MHz, ^{13}C NMR spectra) or on an Agilent/Varian/Chemagnetics InfinityPlus CMX-360 (B_0 = 8.46 T, 115.48 MHz ^{11}B and 36.48 MHz ^{15}N NMR spectra) spectrometer. One-pulse direct-excitation experiments (for ^{11}B) or with cross-polarisation (CP) from the protons and with a CW proton decoupling corresponding to the nutation frequency of protons 76 and 38 kHz (for ^{13}C and ^{15}N, respectively) were carried out. The cross-polarisation contact time was 5 and 3 ms for ^{13}C and ^{15}N, respectively. The samples were packed either in 4 mm (for ^{11}B) or in 7.5 mm (for ^{13}C and ^{15}N) standard ZrO_2 rotors.

All spectra were externally referenced using polycrystalline adamantane (38.48 ppm relative to TMS (0 ppm))[50] for ^{13}C, polycrystalline NH_4Cl (0 ppm)[51] for ^{15}N and a liquid sample of $Et_2O \cdot BF_3$ (0 ppm) for ^{11}B,[49] filled in a small capillary (1 mm in diameter) and inserted in an empty 4 mm rotor to minimize differences in magnetic susceptibilities between powder samples and the liquid reference.

For ^{11}B, 90°-pulse was 4.4 μs as calibrated using a liquid reference sample of $Et_2O \cdot BF_3$. Then, for solid samples a "quadrupolar" (^{11}B, $I = 3/2$) excitation 45°-pulse of 2.2 μs was used in the one-pulse experiments with a recycling delay of 2 s. Further experimental details are given in the figure legends.

^{15}N chemical shift anisotropy (CSA) parameters δ_{aniso} and η for [EMIm][BScB] were estimated by analysing the intensities of spinning sidebands in the ^{15}N CP/MAS NMR spectral pattern using a simulation program in the Mathematica front end.[52]

The positive and negative ion electrospray mass spectra were obtained with a Micromass Platform 2 ESI-MS instrument.

2.5 Thermal analysis

A Q100 TA instrument was used for differential scanning calorimetric (DSC) measurements to study the thermal behavior of these salts. An average weight of 5–10 mg of each sample was sealed in an aluminium pan and cooled to −120 °C then heated up to 200 °C at a scanning rate of 10.0 °C min^{-1}. Phase transition points for all these salts were read out and tabulated at the onset of each phase transition.

2.6 X-Ray crystallography

The reflection intensity data were measured on a Bruker H8 APEX KAPPA CCD single crystal X-ray diffractometer using graphite-monochromated Mo KR radiation (λ = 0.71073 Å). Crystals were coated with Paratone N oil (Exxon Chemical Co., TX, USA) immediately after isolation and cooled in a stream of nitrogen vapor on the diffractometer. Structures were solved by direct methods using the program SHELXS-93 and refined by full matrix least-squares refinement on $F2$ using SHELXL-97.[53] All non-H atoms were initially located in a difference Fourier map. Thereafter, all non-H atoms, except those for the disordered atoms, were placed in geometrically fixed idealised positions and constrained to ride on their parent atoms with C–H distances in the range 0.95–1.00 Å and $U_{iso}(H) = xU_{eq}(C)$, where x = 1.5 for methyl and 1.2 for all other atoms. Two positions were found for all carbons and oxygens, for the disordered choline cation, while only one position was identified for the nitrogen N2. The disordered atoms were modelled with a s.o.f. of 0.5 with two separate parts identified.†

3. Results and discussion

Five different halogen-free salts comprised of two different chelated orthoborate anions (bis(mandelato)borate, $[BMB]^-$ and bis(salicylato)borate, $[BScB]^-$) and three different nitrogen based cations (choline, $[Chol]^+$; 1-ethyl-2,3-dimethylimidazolium, $[EMIm]^+$; and *N*-ethyl-*N*-methylpyrrolidinium, $[EMPy]^+$) were synthesised by the metathesis reaction of the chloride or iodide salts of cations with lithium orthoborates. One system, [EMPy][BScB], has melting point above 100 °C (t_m = 125 °C) and, therefore, it cannot be classified as an ionic liquid but as a salt with a low melting point. The structures and abbreviations of these cations and anions of the five orthoborate ionic liquids or/and salts are shown in Scheme 1.

3.1 Thermal analysis

The phase behaviour for orthoborate ionic liquids and salts was investigated by differential scanning calorimetry (DSC), and their glass transition temperatures (t_g), crystallisation temperatures (t_c), solid–solid phase transition temperatures (t_{s-s}) and melting points (t_m) are tabulated in Table 1. DSC traces of these ionic liquids and salts are shown in Fig. 1. Among systems with $[BScB]^-$ under study, [Chol][BScB] has the lowest glass transition temperature (−15 °C), and melting transition with onset at *ca.* 90 °C. [EMPy][BScB] also displays a low temperature glass transition at −12 °C, a crystallisation point at 34 °C (an exothermic phase transition) followed by a solid–solid phase transition at 83 °C and, finally, a broad melting transition with onset at 125 °C. The DSC trace of [EMIm][BScB] shows a glass transition at −7 °C, a solid–solid transition at 61 °C, followed by a broad melting transition with onset at *ca.* 90 °C. [EMPy][BMB]

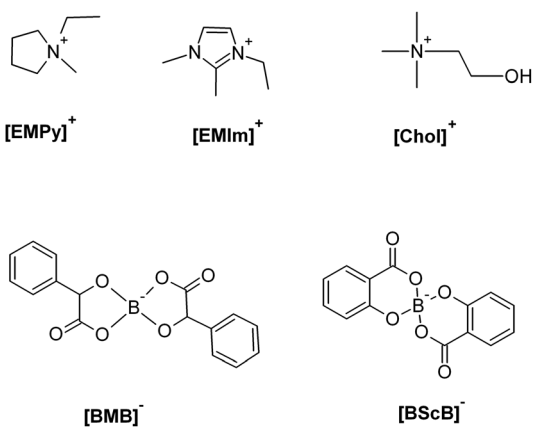

Scheme 1 Structures and abbreviations of anions and cations of ionic liquids and salts investigated.

Table 1 Thermal properties of orthoborate ionic liquids and plastic crystals

Salt	t_g[a]/°C	t_c[b]/°C	$t_{s\text{-}s}$[c]/°C	t_m[d]/°C
[Chol][BScB]	−15			90[e]
[EMPy][BScB]	−12	34	83	125
[EMIm][BScB]	−7		61	90
[EMPy][BMB]	−2			
[EMIm][BMB]	−18			

[a] Glass transition temperature. [b] Crystallisation temperature. [c] Solid–solid phase transition. [d] Onset of melting. [e] Multiple transitions.

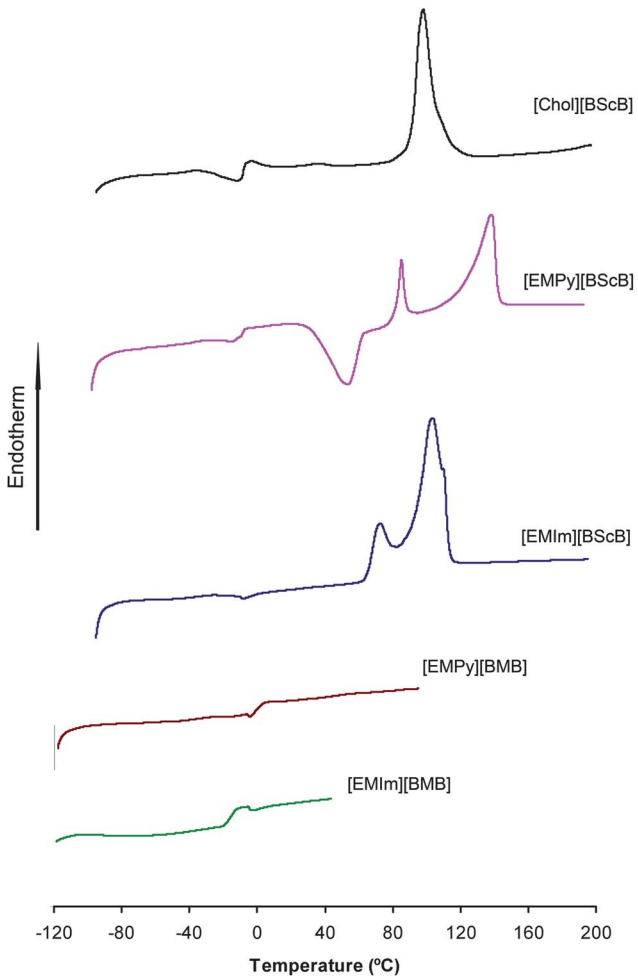

Fig. 1 DSC thermograms of orthoborate ionic liquids at a heating rate of 10 °C min^{-1}.

and [EMIm][BMB] are viscous liquids at room temperature and exhibit only glass transitions at −2 and −18 °C, respectively.

Generally, the phase behaviour of ionic liquids is governed by the nature of both cations and anions, *i.e.* by their intermolecular forces, molecular symmetry and conformational degrees of freedom of the ions.[54] The salts with $[BScB]^-$ anions are solids, while salts with $[BMB]^-$ anions are viscous liquids at room temperature. Note that the $[BMB]^-$ anion is more bulky and with freely rotating phenyl groups compared to the $[BScB]^-$ anion, in which phenyl groups are π-conjugated with carbonyl carbons (see Scheme 1). For salts with the $[BScB]^-$ anion, onset temperatures of melting increase in the order $[Chol]^+ \approx [EMIm]^+ < [EMPy]^+$, where $[EMPy]^+$ is the least bulky cation in this series (see Table 1 and Scheme 1). It is worth noting that two systems, [EMPy][BScB] and [EMIm][BScB], undergo solid–solid phase transitions before reaching their melting points (see Fig. 1 and Table 1). This is a typical characteristic of plastic crystals, in which the rotational motion of one or both of the ions in their lattice sites in the crystal is released above t_{s-s}. This thermal behaviour is rather common for systems based on pyrrolidinium cations with different anions.[55–57] Studies on organic plastic crystals with $[BF_4]^-$ and other fluorine containing anions showing solid–solid phase transitions before melting have also been reported.[58,59]

3.2 Structural description of [Chol][BScB]

A crystal suitable for single-crystal X-ray diffraction was grown by slow evaporation of CH_2Cl_2 from a concentrated solution of [Chol][BScB]. Although the resultant structure is quite disordered, distinct intermolecular interactions may be seen, thus gaining insight into the structure of these salts. A summary of the single crystal data and results of refinement are tabulated in Table 2. The asymmetric unit of [Chol][BScB] consists of two crystallographically independent $[Chol]^+$ cations, one of which is distorted, and two $[BScB]^-$ anions, both of which lie in general positions. The bond distances and angles of the non-disordered $[Chol]^+$ cation and both $[BScB]^-$ anions are all within the normal range (see Fig. S21 in the ESI†). The disordered cation displays two unusually short and long bond lengths brought about by the disorder. The hydroxy-ethyl substituents in the $[Chol]^+$ cation adopts the energetically unpreferred *gauche* conformation (torsional angle N1–C4–C5–O1: −66.8°, N2–C9B–C10B–O2B: −80.1°, N2–C9–C10–O2: 87.4°) and the trimethylammonium substituent adopts the tetrahedral conformation. The $[BScB]^-$ anions display two planar segments joined by the boron atom in a twisted arrangement that results in the two planar segments essentially perpendicular to each other (average O–B–O angle, 108°). The extended structure packs in layers of groups of anions and cations (see Fig. 2a), which result in hydrogen bonded (O–H···O and C–H···π, see Tables 3 and 4) clusters of two cations

Table 2 Summary of crystallographic data and results of refinement for [Chol][BScB] crystal

CCDC no.	809334
Formula	$2(C_{14}H_8BO_6)\cdot C_5H_{14}NO\cdot C_5H_{14}NO$
Molecular weight	760.26
Crystal system	Monoclinic
Space group	*Pc*
a/Å	9.759 (4)
b/Å	16.442 (7)
c/Å	12.446 (5)
B	110.435 (11)°
V/Å^3	1871.5 (13)
Z	2
ρ_{calcd}/g cm^{-1}	1.349
T/K	123
μ/mm^{-1}	0.10
λ/Å	0.71073
w$R(F^2)$	0.233

and two anions forming distinct channels. The structure of [Chol][BScB] exhibits strong hydrogen bonding between the OH group of the $[Chol]^+$ cation and the oxygen of the $[BScB]^-$ anion (see Fig. 2b). Several strong inter-anionic and cationic O–H···O and C–H···O hydrogen bonds occur resulting in interconnected ionic clusters. C–H···π contacts are also seen, thus, facilitating the orientation of the spiro anion. A similar hydrogen bonding pattern has been suggested to play an important role in the structure and behaviour of other choline based salts.[60,61]

3.3 Solid-state multinuclear NMR measurements

Solid-state multinuclear, ^{13}C, ^{11}B and ^{15}N MAS NMR spectroscopy was used to characterise structures and to investigate interactions between cations and anions in salts, which are solids at room temperature. Salts carrying the same anion, $[BScB]^-$, but different cations, $[Chol]^+$, $[EMPy]^+$ and $[EMIm]^+$, were interesting systems to investigate the association of $[BScB]^-$ anions with different cations: $[BScB]^-$ anions and $[EMIm]^+$ cations are aromatic, $[EMPy]^+$ cations are non-aromatic but cyclic, while $[Chol]^+$ cations are neither aromatic nor cyclic.

Fig. 3 shows ^{13}C CP/MAS NMR spectra of [Chol][BScB] (Fig. 3a), [EMPy][BScB] (Fig. 3b) and [EMIm][BScB] (Fig. 3c) with suggested assignment of resonance lines.

Resonance lines at 163–166 ppm in ^{13}C CP/MAS NMR spectra of these salts are assigned to carbon sites in carbonyl groups [–C(O)–], while resonance peaks at 158–160 ppm are due to the carbon sites in phenyl rings directly bonded to the oxygen atoms. There are two resonance lines for the carbon atom of the carbonyl group in [Chol][BScB], while a single line is observed for the same carbon atom in [EMPy][BScB]. Similarly two resonance lines in [Chol][BScB] are assigned to the aromatic carbon atom of the phenyl group directly attached to the oxygen atom, while a single resonance is observed for the same carbon site in the case of [EMPy][BScB]. A similar pattern is observed for other aromatic carbon sites of phenyl groups in $[BScB]^-$ anions of both [Chol][BScB] and [EMPy][BScB] salts. These data suggest a strong interaction between $[Chol]^+$ cation and $[BScB]^-$ anions that makes carbon sites in the $[BScB]^-$ anion chemically inequivalent in the case of the [Chol][BScB] ionic liquid. This interaction is due to the C–H···π interaction and strong hydrogen bonds between the OH groups of $[Chol]^+$ cations and oxygen atoms of $[BScB]^-$ anions. This is in accord with the single crystal molecular structure of [Chol][BScB] as described above (see Fig. 2).

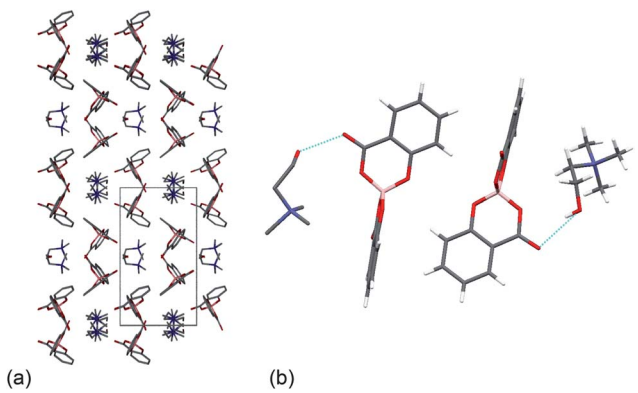

Fig. 2 A packing diagram of [Chol][BScB] viewed down the *c*-axis showing the packed layers (a). Molecular structure of [Chol][BScB] inter-ionic dimer, showing the OH···O hydrogen bonding between cations and anions (b).

Table 3 Hydrogen-bond geometry (Å, °) in [Chol][BScB] crystal[a]

D–H···A	D–H	H···A	D···A	D–H···A
O1–H1···O8A^{i}	0.84	2.41	3.105 (8)	141
O1–H1···O11A^{i}	0.84	2.19	2.916 (8)	145
C1–H1B···O1^{ii}	0.98	2.46	3.390 (11)	158
C1–H1*C*···O2A	0.98	2.57	3.534 (11)	170
C2–H2*C*···O12A	0.98	2.41	3.315 (11)	153
C3*–H3*C*···O1	0.98	2.47	3.048 (11)	117
C3–H3*C*···O12A^{iii}	0.98	2.55	3.292 (11)	133

[a] Symmetry codes: (i) $x + 1, y, z$; (ii) $x, -y + 1, z + 1/2$; (iii) $x, -y + 1, z - 1/2$.

When a ^{13}C CP/MAS NMR spectrum of [EMIm][BScB] is compared with ^{13}C CP/MAS NMR spectra of [Chol][BScB] and [EMPy][BScB], substantial differences in the resonance pattern of $[BScB]^-$ anions can be noticed (see Fig. 3c). Several broad resonance lines for each carbon site, overlapping with one another, are observed for both $[BScB]^-$ anion and $[EMIm]^+$ cation that suggests structural inequivalence of both cations and anions in this system. However, more studies are needed in order to distinguish between intra- and intercrystalline molecular polymorphism and to investigate interactions of $[EMIm]^+$ cations with the $[BScB]^-$ anions in this salt in detail.

Fig. 4 shows ^{11}B single pulse MAS NMR spectra of [Chol][BScB] (Fig. 4a), [EMPy][BScB] (Fig. 4b) and [EMIm][BScB] (Fig. 4c). The ^{11}B NMR spectra reveal single resonance lines for [Chol][BScB] at 3.5 ppm and for [EMPy][BScB] at 3.4 ppm, while two resonance lines for [EMIm][BScB] at 3.4 and 2.8 ppm. These chemical shifts confirm four-coordinated boron units in all these anions.[62] A slightly downfield shift (0.1 ppm) towards higher δ-values is observed in the ^{11}B MAS NMR of [Chol][BScB]. This means that boron site in [Chol][BScB] is slightly less shielded compared to the boron sites in [EMPy][BScB] and [EMIm][BScB]. The two ^{11}B resonance lines assigned to the $[BScB]^-$ anions in [EMIm][BScB] suggest the presence of two different forms of four-coordinated boron sites and a structural inequivalence of $[BScB]^-$ anions in this system as also observed in ^{13}C CP/MAS NMR spectra of [EMIm][BScB] discussed above.

Fig. 5 shows ^{15}N CP/MAS NMR spectra of [EMPy][BScB] (Fig. 5a) and [Chol][BScB] (Fig. 5b). The ^{15}N CP/MAS NMR spectra of [Chol][BScB] and [EMPy][BScB] reveal single sharp resonance lines at 34.5 and 9.2 ppm, respectively.

Table 4 Geometrical parameters (Å, °) of selected inter-ring C–H···π interactions in [Chol][BScB] crystal. The CgJ refers to the ring centre-of-gravity[a]

X–H/X	CgJ	H···Cg	X–H···Cg	X···Cg	Symmetry position of CgJ
C19A–H19A	Cg1	2.87	141	3.066 (10)	*x*,*y*,*z*

[a] *Note*: Cg1 is the centroid of ring C2A/C3A/C4A/C5A/C6A/C7A.

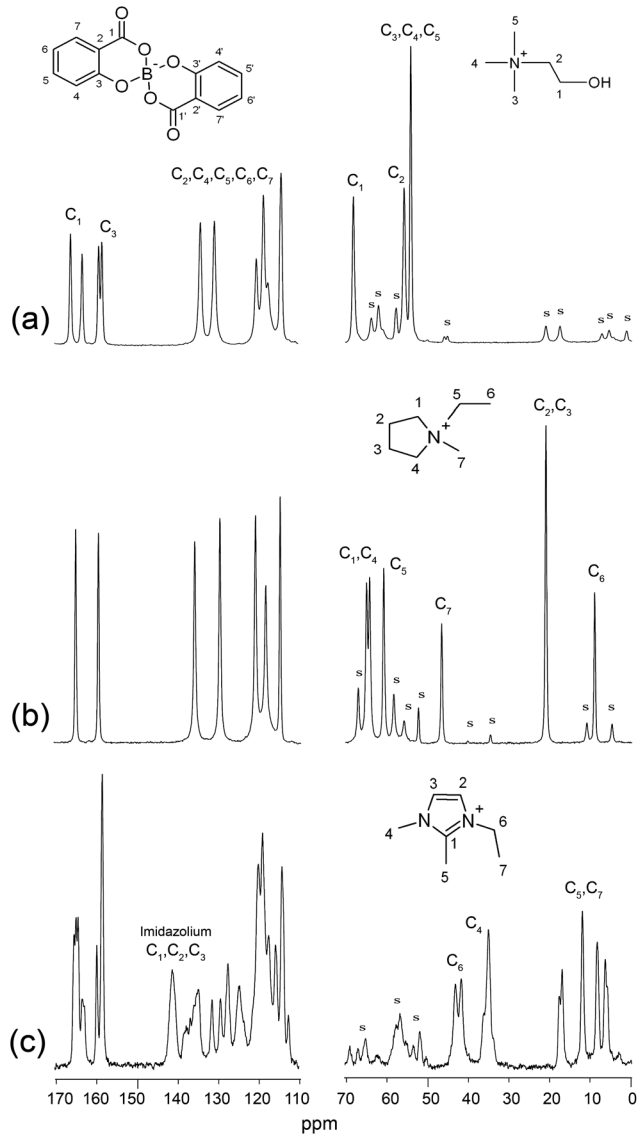

Fig. 3 ^{13}C CP/MAS NMR spectra of polycrystalline [Chol][BScB] (a), [EMPy][BScB] (b), and [EMIm][BScB] (c). The MAS frequency was 4.2 kHz in (a), 4.7 kHz in (b) and (c). 1024 signal transients were accumulated in (a) and (b), and 852 signal transients were co-added in (c). "s" denotes spinning sideband. The spinning sidebands between 70 and 110 ppm are omitted for clarity.

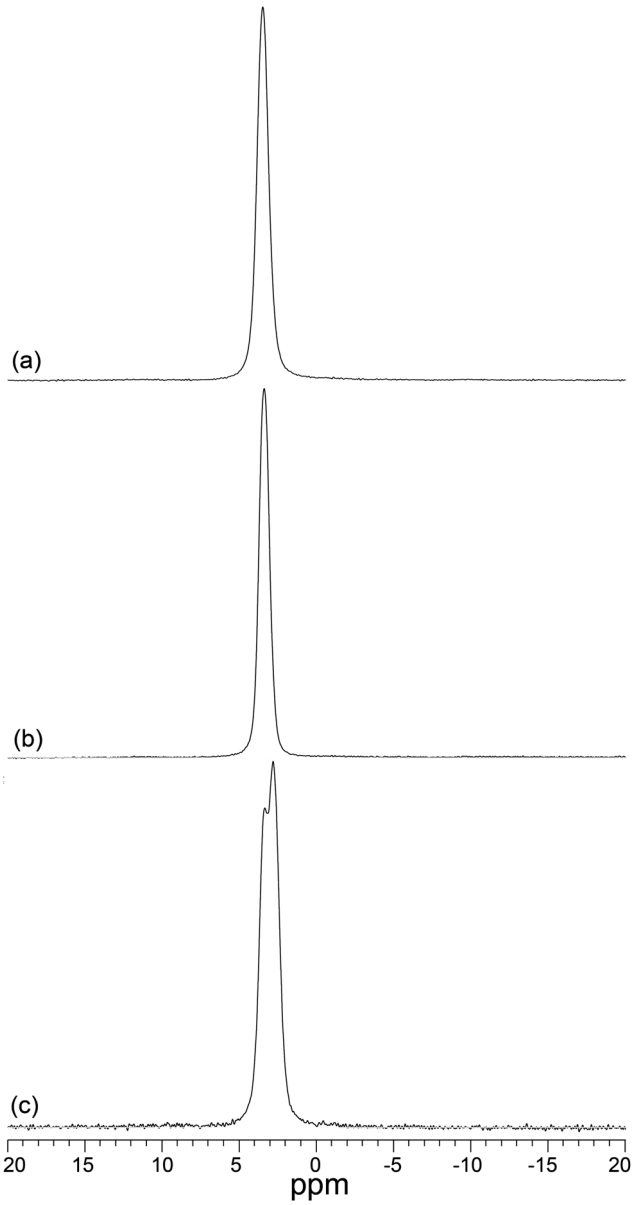

Fig. 4 ^{11}B MAS NMR spectra of polycrystalline [Chol][BScB] (a), [EMPy][BScB] (b), and [EMIm][BScB] (c). The MAS frequency was 13 kHz. 64 signal transients were co-added in (a) and (b), and 1280 signal transients were accumulated in (c).

^{15}N CP/MAS NMR spectrum of [EMIm][BScB] is shown in Fig. 6. This spectrum displays two resonance lines for each nitrogen atom of $[EMIm]^+$ cations (see the inset in Fig. 6), again suggesting (as ^{11}B MAS and ^{13}C CP/MAS NMR data for the anion) that there are two inequivalent $[EMIm]^+$ cations in this salt. The ^{15}N chemical shifts for the nitrogen sites (average of the two inequivalent nitrogen atoms) together with the ^{15}N chemical shift anisotropy (CSA) data for [EMIm][BScB] are tabulated in Table 5.

The structure of compounds and materials in the solid-state can be significantly different from the structure of these substances in solutions. The molecular properties of a system in the solid state, for example, hydrogen bond arrangements and interactions between aromatic molecular moieties (π stacking), can be readily probed by NMR in the solid state.[63] These interactions in combination with electrostatic and van der Waals forces are of particular interest in ILs, which are solids at room temperature: a spatial arrangement and orientation of ions would strongly depend on these interactions between cations and anions and that, in turn, will influence the macroscopic properties of ILs, such as their density, viscosity, conductivity, phase transition and temperatures.[64]

A number of X-ray diffraction studies have been employed for the structural analysis of imidazolium halides and related salts to elucidate the intermolecular interactions between cations and anions.[65–67] These analyses have revealed that both hydrogen bonding and hydrogen-bond-like C–H···anion interactions

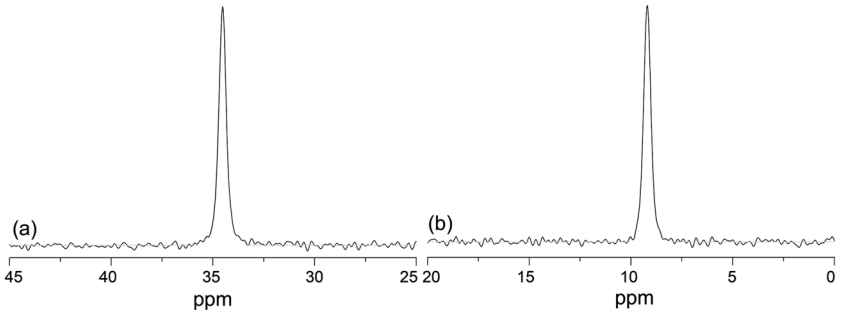

Fig. 5 Natural abundance ^{15}N CP/MAS NMR spectra of polycrystalline [Chol][BScB] (a) and [EMPy][BScB] (b). The MAS frequency was 2.0 kHz in (a) and 2.1 kHz in (b). 15 368 and 18 060 signal transients were accumulated in (a) and (b), respectively.

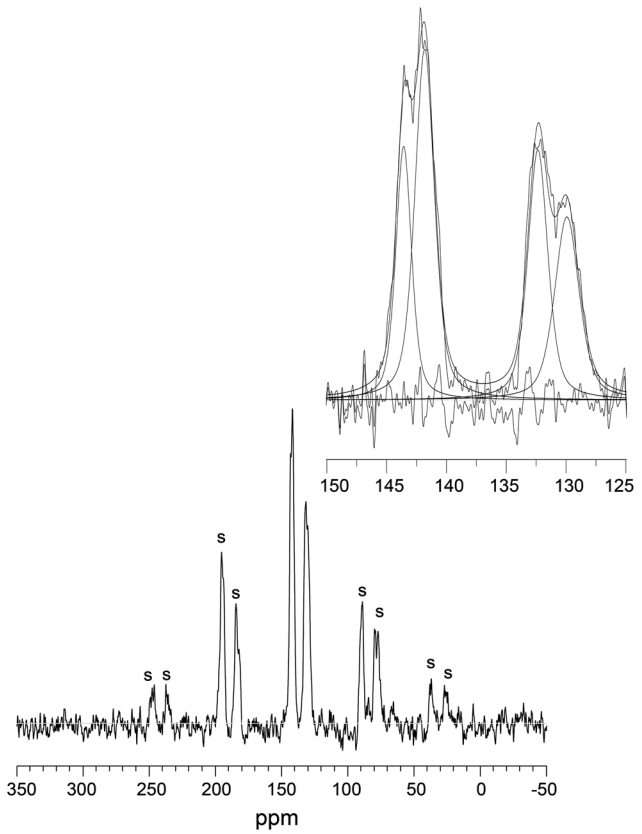

Fig. 6 Natural abundance ^{15}N CP/MAS NMR spectrum of polycrystalline [EMIm][BScB]. The MAS frequency was 1.9 kHz and 26 324 signal transients were accumulated. "s" represents spinning sidebands. The expanded center-band region with deconvolutions is shown in the inset.

Table 5 ^{15}N chemical shifts and chemical shift anisotropy (CSA) data for [EMIm][BScB]

Salt	δ_{iso}/ppm	δ_{aniso}/ppm	η_{cs}
[EMIm][BScB]	142.8	-109.9 ± 1.4	0.61 ± 0.05
	131.3	-102.8 ± 1.9	0.92 ± 0.06

between cations and anions govern polymorphism in these salts. Holbrey *et al.* have reported on the presence of two crystalline polymorphs, with orthorhombic and monoclinic symmetry, for 1-butyl-3-methylimidazolium chloride studied by single crystal X-ray diffraction at -100 °C.[68] Interactions between cations and anions in imidazolium based ILs have been also studied by FTIR spectroscopy.[69–72] It has been suggested that imidazolium cations form hydrogen bonds with bis(trifluoromethylsulfonyl)imide anions, $[NTf_2]^-$, in this type of ILs. Recently, Cremer *et al.* have employed liquid-state NMR spectroscopy in combination with X-ray photoelectron spectroscopy (XPS) to probe cation–anion interactions in neat room temperature imidazolium based ILs and these authors have also suggested that hydrogen-bond-like C–H···anion interactions are present in these ILs and strongly influence on their properties.[73]

Multinuclear solid-state NMR measurements in this study suggest that interactions between $[BScB]^-$ anions and the different nitrogen based cations strongly depend on the nature of cations. Unlike the room temperature orthoborate–phosphonium ILs,[41] orthoborate salts with nitrogen-based cations are either solid and/or viscous liquids at room temperature. We suggest that this is due to more compact structures, with shorter alkyl chains on the nitrogen atoms, of cations used in this study. In addition, the OH groups of $[Chol]^+$ cations form hydrogen bonds with carbonyl oxygen atoms of $[BScB]^-$ anions in [Chol][BScB] that additionally elevates the melting point of this IL. These hydrogen bonds were clearly detected in the single crystal structure of [Chol][BScB] (see Fig. 2) and further supported by ^{13}C CP/MAS NMR (Fig. 3a): the two phenyl rings in the $[BScB]^-$ anion are chemically inequivalent that gives rise to two well-resolved resonance lines in the ^{13}C CP/NMR spectrum for carbon sites in both carbonyl and phenyl groups of $[BScB]^-$. Interestingly, both ^{11}B MAS NMR and ^{15}N CP/MAS NMR spectra of this salt revealed single resonance lines for both boron and nitrogen sites which suggests the chemical equivalence of anions (from ^{11}B NMR and confirmed by X-ray diffraction) as well as for the $N(CH_3)_3$ groups of the two cations in the unit cell of [Chol][BScB] (from ^{15}N NMR).

Multinuclear ^{13}C, ^{11}B and ^{15}N solid-state NMR on [EMIm][BScB] have revealed polymorphism in this salt, which is most probably due to the presence of strong $\pi\cdots\pi$ stacking and C–H$\cdots\pi$ interactions between the imidazolium cations and the phenyl groups of $[BScB]^-$ anions as in previously reported 1-*n*-butyl-3-methylimidazolium tetraphenylborate ionic liquids.[74,75] X-ray diffraction studies have shown both $\pi\cdots\pi$ stacking and C–H$\cdots\pi$ interactions between the imidazolium cations and the phenyl groups of tetraphenylborate anions.[74,75] These X-ray

diffraction studies have suggested that hydrogen atoms of the imidazolium ring form three-dimensional networks through weak C–H···π bonds and this type of supramolecular structure is maintained both in solid state and possibly even in chloroform solutions of this type of ILs. The two resolved resonance lines in both ^{11}B MAS NMR and ^{15}N CP/MAS NMR spectra of polycrystalline [EMIm][BScB] suggest that two polymorphs are present in the structure of this salt. In addition, DSC data for this system (see Fig. 1) also revealed a broad peak for the phase transition of melting with a small shoulder at higher temperature that suggests melting of two different polymorphs having slightly different melting points.

In contrast to other systems under study, ^{13}C, ^{11}B and ^{15}N MAS NMR reveal sharp single resonance lines for carbon, boron and nitrogen sites in the [EMPy][BScB] salt that suggests that there are no pronounced hydrogen bonds, π···π stacking or C–H···π interactions between $[EMPy]^+$ cations and $[BScB]^-$ anions, which may lead to a structural polymorphism in the [EMPy][BScB] system. It can be suggested that a lack of such interactions is probably due to the lack of OH groups, aromaticity and/or conjugated π bonds in the pyrrolidinium cations. These two systems, [EMIm][BScB] and [EMPy][BScB], will be further studied by X-ray diffraction crystallography upon obtaining single crystals suitable for this method and results will be reported elsewhere.

Recent studies have shown that some ILs can form complexes with lanthanide ions.[76,77] We also found that lanthanide(III) ions can be successfully extracted from aqueous solution by using [Chol][BScB] at elevated temperatures just above the melting point of this IL (+95 °C) but below the boiling point of water.

Based on ^{13}C and ^{11}B MAS NMR and ICP-SFMS elemental analysis data, we suggest that $[BScB]^-$ anions strongly interact with La^{3+}(aq) ions resulting in the formation of $La_x[BScB]_y$ complexes, which precipitate from aqueous solutions. A ^{11}B MAS NMR spectrum of the $La_x[BScB]_y$ precipitate has revealed a single resonance line at 4.4 ppm assigned here to four-coordinated boron sites in this complex, which is additionally deshielded (by 0.9 ppm) as compared to pure IL [Chol][BScB] with the single resonance line at 3.5 ppm (see Fig. 7).

A ^{13}C CP/MAS NMR spectrum of this precipitate showed resonance lines between 118 and 177 ppm, which can be assigned to the aromatic and carbonyl groups of $[BScB]^-$ anions (see Fig. S25 in the ESI†). No resonance lines were observed for aliphatic carbons in this spectrum, which proves that $[Chol]^+$ was left in the aqueous phase after the extraction process. Further studies to obtain suitable single crystals of $La_x[BScB]_y$, to prove the proposed complex-formation mechanism and to evaluate affinities of boron-based ionic liquids to other rare earth elements are currently in progress.

4. Conclusions

This work reports on the preparation of five halogen-free orthoborate ionic liquids with cholinium, pyrrolidinium and imidazolium as cations and two chelated orthoborate anions, bis(mandelato)borate and bis(salicylato)borate. Salts with $[BMB]^-$ anions are viscous liquids at room temperature with glass transition temperatures below 0 °C (−2 and −18 °C for [EMPy][BMB] and [EMIm][BMB], respectively). The other three

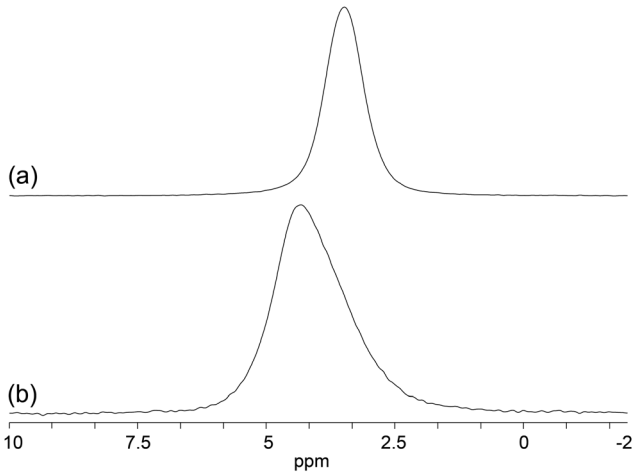

Fig. 7 ^{11}B MAS NMR spectra of polycrystalline [Chol][BScB] (a) and a powder lanthanum complex with bis(salicylato)borate after the extraction process of La^{3+}(aq) by [Chol][BScB] (b). The MAS frequency was 13 kHz. 64 and 1200 signal transients were accumulated in (a) and (b), respectively.

salts with $[BScB]^-$ anions are all solids at room temperature showing both melting (around 90–125 °C) and glass transitions (between −15 and −7 °C). [EMPy][BScB] and [EMIm][BScB] may be classified as plastic crystals, since they have solid–solid phase transitions before melting. Onset temperatures of melting of the salts with the $[BScB]^-$ anion and different cations increase in the order $[Chol]^+ \approx [EMIm]^+ < [EMPy]^+$.

Using solid-state multinuclear NMR it was found that ^{13}C chemical shifts of the carbonyl and the phenyl carbon sites in $[BScB]^-$ anions are significantly influenced, while ^{11}B chemical shifts are weakly influenced by the hydrogen bonding, π···π and C–H···π interactions between the anion and $[Chol]^+$ and $[EMIm]^+$ cations in these salts, which are solids at room temperature. ^{13}C, ^{11}B and ^{15}N solid-state NMR data suggest that these interactions are not present in [EMPy][BScB], probably because of the lack of aromaticity in $[EMPy]^+$. Combined ^{13}C, ^{11}B and ^{15}N solid-state NMR data also suggest that solid [EMIm][BScB] has two coexisting polymorphs at room temperature. Single crystal X-ray diffraction of [Chol][BScB] revealed hydrogen bonding between OH of two structurally inequivalent $[Chol]^+$ cations and carbonyl groups of structurally equivalent $[BScB]^-$ anions in the unit cell of $2[BScB]^-\cdot[Chol]^+\cdot[Chol]^+$. Extraction experiments showed that [Chol][BScB] can be successfully used for the extraction of lanthanum(III) cations from aqueous solution. It was found that a lanthanum complex with bis(salicylato)borate has readily precipitated from a liquid mixture of La^{3+}(aq) with [Chol][BScB] at 95 °C suggesting that among other future applications these novel ILs can be potentially used in the extraction processes of metal ions of rare earth elements.

Acknowledgements

The financial support (a stipend for FUS) provided by the Foundation in memory of J. C. and Seth M. Kempe and Swedish Research School in Tribology are gratefully acknowledged. MF and DRM are grateful for the support of the Australian

Research Council under its Discovery Projects and Federation Fellowship (DRM) schemes. Dr Jiazeng Sun is acknowledged for all help with the synthesis and characterisation of ionic liquids. We also thank Dr Anna-Carin Larsson for her assistance with the ^{15}N CSA analysis. An Agilent/Varian/Chemagnetics InfinityPlus CMX-360 NMR spectrometer at LTU has been purchased with a grant from the Swedish Council for Planning and Coordination of Research (FRN) and further upgraded with JCK-2003, JCK-2307 and JCK-2905 grants from the Foundation in memory of J. C. and Seth M. Kempe. Solid-state ^{13}C CP/MAS NMR experiments were performed on an Agilent/Varian/Chemagnetics InfinityPlus CMX-300 NMR spectrometer in the Magnetic Resonance laboratory at the University of Warwick, while all liquid state NMR experiments were carried out on a Bruker Avance 400 NMR spectrometer at Monash University.

References

1 N. V. Plechkova and K. R. Seddon, *Chem. Soc. Rev.*, 2008, **37**, 123–150.
2 R. D. Rogers and K. R. Seddon, *Science*, 2003, **302**, 792–793.
3 R. D. Rogers, *Nature*, 2007, **447**, 917–918.
4 K. Tsunashima, E. Niwa, S. Kodama, M. Sugiya and Y. Ono, *J. Phys. Chem. B*, 2009, **113**, 15870–15874.
5 T. Torimoto, T. Tsuda, K. Okazaki and S. Kuwabata, *Adv. Mater.*, 2010, **22**, 1196–1221.
6 S. T. Handy and M. Okello, *J. Org. Chem.*, 2005, **70**, 2874–2877.
7 B. C. Ranu and S. Banerjee, *Org. Lett.*, 2005, **7**, 3049–3052.
8 Y. Gu, J. Zhang, Z. Duan and Y. Deng, *Adv. Synth. Catal.*, 2005, **347**, 512–516.
9 R. J. Brown, P. J. Dyson, D. Ellis and T. Welton, *Chem. Commun.*, 2001, 1862–1863.
10 F. Shi, Y. Deng, T. SiMa, J. Peng, Y. Gu and B. Qiao, *Angew. Chem., Int. Ed.*, 2003, **42**, 3257–3260.
11 D. R. MacFarlane, M. Forsyth, P. C. Howlett, J. M. Pringle, J. Sun, G. Annat, W. Neil and E. I. Izgorodina, *Acc. Chem. Res.*, 2007, **40**, 1165–1173.
12 L. Jin, P. C. Howlett, J. Efthimiadis, M. Kar, D. R. MacFarlane and M. Forsyth, *J. Mater. Chem.*, 2011, **21**, 10171–10178.
13 V. Armel, D. Velayutham, J. Sun, P. C. Howlett, M. Forsyth, D. R. MacFarlane and J. M. Pringle, *J. Mater. Chem.*, 2011, **21**, 7640–7650.
14 P. Wasserscheid and W. Keim, *Angew. Chem., Int. Ed.*, 2000, **39**, 3772–3789.
15 T. Welton, *Chem. Rev.*, 1999, **99**, 2071–2084.
16 J. Stoimenovski, D. R. MacFarlane, K. Bica and R. D. Rogers, *Pharm. Res.*, 2010, **27**, 521–526.
17 K. D. Weaver, H. J. Kim, J. Sun, D. R. MacFarlane and G. D. Elliott, *Green Chem.*, 2010, **12**, 507–513.
18 P. Nockemann, R. V. Deun, B. Thijs, D. Huys, E. Vanecht, K. V. Hecke, L. V. Meervelt and K. Binnemans, *Inorg. Chem.*, 2010, **49**, 3351–3360.
19 J. S. Wang, C. N. Sheaff, B. Yoon, R. S. Addleman and C. M. Wai, *Chem.–Eur. J.*, 2009, **15**, 4458–4463.
20 S. Chun, S. V. Dzyuba and R. A. Bartsch, *Anal. Chem.*, 2001, **73**, 3737–3741.
21 B. S. Lee, Y. S. Chi, J. K. Lee, I. S. Choi, C. E. Song, S. K. Namgoong and S. Lee, *J. Am. Chem. Soc.*, 2004, **126**, 480–481.
22 M. Cai, Y. Liang, F. Zhou and W. Liu, *J. Mater. Chem.*, 2011, **21**, 13399–13405.
23 Q. Zhang, X. Xiangyuan, S. Liu, B. Yang, L. Lu, Y. He and Y. Geng, *J. Mater. Chem.*, 2011, **21**, 6864–6868.
24 V. A. Cocalia, K. E. Gutowski and R. D. Rogers, *Coord. Chem. Rev.*, 2006, **250**, 755–764.
25 S. Zahn, F. Uhlig, J. Thar, C. Spickermann and B. Kirchner, *Angew. Chem., Int. Ed.*, 2008, **47**, 3639.
26 J. D. Holbrey, W. M. Reichert, M. Nieuwenhuyzen, S. Johnston, K. R. Seddon and R. D. Rogers, *Chem. Commun.*, 2003, 1636–1637.
27 Z. Wei, X. Wei, X. Wang, X. Wang, Z. Wang and J. Liu, *J. Mater. Chem.*, 2011, **21**, 6875–6882.
28 P. A. Hunt, B. Kirchner and T. Welton, *Chem.–Eur. J.*, 2006, **12**, 6762–6775.
29 P. A. Hunt, *J. Phys. Chem. B*, 2007, **111**, 4844–4853.
30 H. Tokuda, S. Tsuzuki, M. Susan, K. Hayamizu and M. Watanabe, *J. Phys. Chem. B*, 2006, **110**, 19593–19600.
31 S. C. Luo, S. Sun, A. R. Deorukhkar, J. T. Lu, A. Bhattacharyya and I. J. B. Lin, *J. Mater. Chem.*, 2011, **21**, 1866–1873.
32 L. Cammarata, S. G. Kazarian, P. A. Salter and T. Welton, *Phys. Chem. Chem. Phys.*, 2001, **3**, 5192–5200.
33 R. P. Swatloski, J. D. Holbrey and R. D. Rogers, *Green Chem.*, 2003, **5**, 361–363.
34 B. Jastorff, R. Stormann, J. Ranke, K. Molter, F. Stock, B. Oberheitmann, W. Hoffmann, J. Hoffmann, M. Nuchter, B. Ondruschka and J. Filser, *Green Chem.*, 2003, **5**, 136–142.
35 P. Wasserscheid, R. van Hal and A. Bosmann, *Green Chem.*, 2002, **4**, 400–404.
36 T. P. T. Pham, C. W. Cho and Y. S. Yun, *Water Res.*, 2010, **44**, 352–372.
37 M. Petkovic, K. R. Seddon, L. P. N. Rebelo and C. S. Pereira, *Chem. Soc. Rev.*, 2011, **40**, 1383–1403.
38 J. Ranke, S. Stolte, R. Störmann, J. Arning and B. Jastorff, *Chem. Rev.*, 2007, **107**, 2183–2206.
39 C. Zhang, S. V. Malhotra and A. J. Francis, *Chemosphere*, 2011, **82**, 1690–1695.
40 K. M. Docherty and C. F. Kulpa, *Green Chem.*, 2005, **7**, 185–189.
41 F. U. Shah, S. Glavatskih, D. R. MacFarlane, A. Somers, M. Forsyth and O. N. Antzutkin, *Phys. Chem. Chem. Phys.*, 2011, **13**, 12856–12873.
42 P. C. Howlett, J. Sunarso, Y. Shekibi, E. Wasser, L. Jin, M. Kar, D. R. MacFarlane and M. Forsyth, *Solid State Ionics*, 2011, **204–205**, 73–79.
43 J. Sunarso, Y. Shekibi, J. Efthimiadis, L. Jin, J. M. Pringle, A. F. Hollenkamp, D. R. MacFarlane, M. Forsyth and P. C. Howlett, *J. Solid State Electrochem.*, 2012, DOI: 10.1007/s10008-011-1566-6.
44 D. R. MacFarlane, P. Meakin, J. Sun, N. Amini and M. Forsyth, *J. Phys. Chem. B*, 1999, **103**, 4164–4170.
45 S. Yu, S. Lindeman and C. D. Tran, *J. Org. Chem.*, 2008, **73**, 2576–2591.
46 W. Xu, L. M. Wang, R. A. Nieman and C. A. Angell, *J. Phys. Chem. B*, 2003, **107**, 11749–11756.
47 http://www.mikrokemi.se.
48 http://www.alsglobal.se.
49 Z. J. A. Komon, J. S. Rogers and G. C. Bazan, *Organometallics*, 2002, **21**, 3189–3195.
50 C. R. Morcombe and K. W. Zilm, *J. Magn. Reson.*, 2003, **162**, 479–486.
51 K. Karaghiosoff, *Encyclopedia of Nuclear Magnetic Resonance*, ed. D. M. Grant and R. K. Harris, Wiley, New York, 1996, vol. 6, p. 3612.
52 O. N. Antzutkin, Y. K. Lee and M. H. Levitt, *J. Magn. Reson.*, 1998, **135**, 144–155.
53 G. M. Sheldrick, *Acta Crystallogr., Sect. A: Found. Crystallogr.*, 2008, **A64**, 112–122.
54 Q. Zhang, S. Liu, Z. Li, J. Li, Z. Chen, R. Wang, L. Lu and Y. Deng, *Chem.–Eur. J.*, 2009, **15**, 765–778.
55 J. Golding, S. Forsyth, D. R. MacFarlane, M. Forsyth and G. B. Deacon, *Green Chem.*, 2002, **4**, 223–229.
56 J. Sun, D. R. MacFarlane and M. Forsyth, *J. Mater. Chem.*, 2001, **11**, 2940–2942.
57 D. R. MacFarlane and M. Forsyth, *Adv. Mater.*, 2001, **13**, 957–966.
58 J. M. Pringle, P. C. Howlett, D. R. MacFarlane and M. Forsyth, *J. Mater. Chem.*, 2010, **20**, 2056–2062.
59 J. M. Pringle, J. Adebahr, D. R. MacFarlane and M. Forsyth, *Phys. Chem. Chem. Phys.*, 2010, **12**, 7234–7240.
60 P. M. Dean, J. Turanjanin, M. Yoshizawa-Fujita, D. R. MacFarlane and J. L. Scott, *Cryst. Growth Des.*, 2009, **9**, 1137–1145.
61 P. Nockemann, B. Thijs, K. Driesen, C. R. Janssen, K. V. Hecke, L. V. Meervelt, S. Kossmann, B. Kirchner and K. Binnemans, *J. Phys. Chem. B*, 2007, **111**, 5254–5263.
62 M. R. Hansen, T. Vosegaard, H. J. Jakobsen and J. Skibsted, *J. Phys. Chem. A*, 2004, **108**, 586–594.
63 H. Erdemi, U. Akbey and W. H. Meyer, *Solid State Ionics*, 2010, **181**, 1586–1595.
64 P. M. Dean, J. M. Pringle and D. R. MacFarlane, *Phys. Chem. Chem. Phys.*, 2010, **12**, 9144–9153.

65 J. D. Holbrey, W. M. Reichert and R. D. Rogers, *Dalton Trans.*, 2004, 2267–2271.
66 A. Downard, M. J. Earle, C. Hardacre, S. E. J. McMath, M. Nieuwenhuyzen and S. J. Teat, *Chem. Mater.*, 2004, **16**, 43–48.
67 W. M. Reichert, J. D. Holbey, R. P. Swatloski, K. E. Gutowski, A. E. Visser, M. Nieuwenhuyzen, K. R. Seddon and R. D. Rogers, *Cryst. Growth Des.*, 2007, **7**, 1106–1114.
68 J. D. Holbrey, W. M. Reichert, M. Nieuwenhuyzen, S. Johnston, K. R. Seddon and R. D. Rogers, *Chem. Commun.*, 2003, 1636–1637.
69 K. Fumino, A. Wulf and R. Ludwig, *Angew. Chem., Int. Ed.*, 2008, **47**, 3830–3834.
70 K. Fumino, A. Wulf and R. Ludwig, *Angew. Chem., Int. Ed.*, 2008, **47**, 8731–8734.
71 K. Fumino, A. Wulf and R. Ludwig, *Angew. Chem., Int. Ed.*, 2009, **49**, 449–453.
72 C. Roth, T. Peppel, K. Fumino, M. Köckerling and R. Ludwig, *Angew. Chem., Int. Ed.*, 2010, **49**, 10221–10224.
73 T. Cremer, C. Kolbeck, K. R. J. Lovelock, N. Paape, R. Wölfel, P. S. Schulz, P. Wasserscheid, H. Weber, J. Thar, B. Kirchner, F. Maier and H. P. Steinruck, *Chem.–Eur. J.*, 2010, **16**, 9018–9033.
74 J. Dupont, P. A. Z. Suarez, R. F. de Souza, R. A. Burrow and J. P. Kintzinger, *Chem.–Eur. J.*, 2000, **6**, 2377–2381.
75 C. S. Consorti, P. A. Z. Suarez, R. F. de Souza, R. A. Burrow, D. H. Farrar, A. J. Lough, W. Loh, L. H. M. da Silva and J. Dupont, *J. Phys. Chem. B*, 2005, **109**, 4341–4349.
76 J. H. Olivier, F. Camerel and R. Ziessel, *Chem.–Eur. J.*, 2011, **17**, 9113–9122.
77 A. I. Bhatt, I. May, V. A. Volkovich, D. Collison, M. Helliwell, I. B. Polovo and R. G. Lewin, *Inorg. Chem.*, 2005, **44**, 4934–4940.

